Dalton Transactions

Accepted Manuscript

ROYAL SOCIETY OF CHEMISTRY

www.rsc.org/dalton

Dalton Transactions

RSCPublishing

ARTICLE

Cobalt and copper pyridylmethylphosphonates with two- and three-dimensional structures and field-induced magnetic transitions

Ting-Hai Yang,[a,c,d] Zhong-Sheng Cai,[c] Fa-Nian Shi*[b,d] and Li-Min Zheng*[c]

Cite this: DOI: 10.1039/x0xx00000x

Received 00th January 2015,
Accepted 00th January 2015

DOI: 10.1039/x0xx00000x

www.rsc.org/

Two novel metal pyridylmethylphosphonates, namely, [Co(4-pmp)] (**1**) and [Cu(4-pmp)(H_2O)] (**2**), (4-pmpH_2 = 4-pyridylmethylphosphonic acid), have been hydrothermally synthesized and characterized by X-ray diffraction, infrared spectroscopy, elemental analysis, thermogravimetric analysis. In compound **1**, each {PO_3C} tetrahedron is corner-shared with three {$CoNO_3$} tetrahedra and vice versa, thus forming a one-dimensional (1-D) inorganic chain along the *a* axis containing 8-membered rings of [(Co–O–P–O)$_2$]. The inorganic chains are further connected by 4-pmp^{2-} ligand, generating a 2-D layered structure. Compound **2** displays a three-dimensional (3-D) framework structure, in which the inorganic layers are pillared by the pyridyl groups of the ligand, generating a 3-D pillared-layered structure. The magnetic properties of **1** and **2** have been studied. Compounds **1** and **2** behave as metamagnets at low temperature. The critical fields are about 70 kOe for **1** and 47 kOe for **2** at 1.8 K.

Introduction

The chemistry of metal phosphonates has gained an increasing attention in recent years.[1, 2] The great interest in this area is driven not only by their aesthetically beautiful architectures and topologies[3,4] but also their potential applications in sorption,[5-7] catalysis,[8-11] proton conductivity,[12-16] optics[17-19] and magnetism. In the study of molecule-based magnetic materials, metal phosphonates could provide good examples for understanding some interesting magnetic phenomena, for example, single molecule magnets,[20-30] single chain magnets,[31-35] ferrimagnetism,[36-40] weak ferromagnetism,[41-45] field-induced transition,[49-56] etc. However, the number of metal phosphonates exhibiting these magnetic phenomena is limited. Therefore, it is still a great challenge to prepare new metal phosphonates with interesting magnetic properties. Among the various approaches to obtain metal phosphonates, the most efficient one is to employ suitable phosphonic acid ligand, which resulted in a variety of structures with related physical properties.

Pyridylmethylphosphonic acid is one of the excellent N/O mixed ligands for construction of coordination polymers due to their unique coordination behaviors that are resulted from multiple coordination sites involving one pyridine nitrogen and three phosphonate oxygen atoms. To the best of our knowledge, only a limited number of metal phosphonates[51, 53, 57-61] based on 2/3/4-pyridylmethylphosphonic acid (2/3/4-pmpH_2) have been reported. Based on 2-pmpH_2, we succeeded in synthesizing several metal phosphonates with interesting magnetic behaviors, including [Co(2-pmp)(H_2O)][51] and [Mn(2-pmp)(H_2O)$_2$]·H_2O,[53] showing reversible change in both structures and metamagnetic behaviors upon dehydration-hydration process. It has been well known that the formation of a particular structure is dependent not only on the properties of metal ions but also on the properties of ligands including the substitution position of pyridyl groups. In order to investigate the effect of the phosphonates group position on structures and magnetic property of compounds, we select 4-pyridylmethylphosphonic (4-pmpH_2) (Scheme 1) to react with cobalt and copper salts under hydrothermal conditions. Two different structure compounds with formulae [Co(4-pmp)] (**1**) and [Cu(4-pmp)(H_2O)] (**2**) are obtained due to the coordination modes change. Their magnetic properties are investigated showing that they exist as a metamagnetism at low temperature.

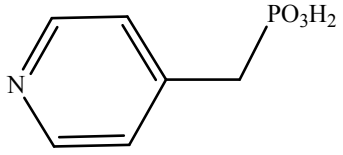

Scheme 1 Chemical structure of 4-pmpH_2 ligand.

Experimental

Materials and methods

All the starting materials were of reagent quality and were obtained from commercial sources without further purification. Elemental analyses for C, N and H were performed on a TruSpec 630-200-200 elemental analyser with a combustion furnace temperature of 1075 °C and an afterburner temperature of 850 °C. FT-IR spectra were collected from KBr pellets (Aldrich 99%+, FT-IR grade) on a Mattson 7000 FT-IR spectrometer in a range of 4000–400 cm^{-1} at the resolution of 2 cm^{-1}. Thermogravimetric analyses (TGA) were carried out using a Shimadzu TGA 50 under air, from room temperature to ca. 700 ºC, with a heating rate of 10 ºC/min. Powder X-ray diffraction (PXRD) patterns were recorded at ambient temperature using an Empyrean diffractometer with Cu-Kα radiation (λ = 1.54178 Å) in the 2θ range of 5 to 50° in reflection mode, which is equipped with a X'Celerator detector, a curved graphite-monochromated radiation and a flat-plate sample holder, in a Bragg-Brentano para-focusing optics configuration (45 kV, 40 mA). Magnetic susceptibility was measured on polycrystalline samples by using a Quantum Design MPMS SQUID VSM system.

Synthesis of [Co(4-pmp)] (1)

A mixture of $Co(OAc)_2 \cdot 4H_2O$ (0.1 mmol, 0.0250 g) and 4-pmpH_2 (0.1mmol, 0.0172 g) in 8 mL H_2O was kept in a Teflon-lined autoclave at 140 °C for 72 h. After the autoclave is cooled to room temperature, blue needle-like crystals of compound **1** were collected as a single phase, judging by the powder-X-ray diffraction (PXRD) measurement. Yield: 10.6 mg (46% based on 4-pmpH_2). Elemental anal. calcd. for $C_6H_6NO_3PCo$: C, 36.20; H, 3.04; N, 7.04%. Found: C, 36.35; H, 3.11; N, 6.98%. IR (KBr, cm^{-1}): 1613(s), 1556(w), 1507(w), 1432(m), 1242(m), 1220(m), 1210(m), 1125(s), 1090(s), 1057(s), 1028(m), 997(s), 859(m), 837(m), 765(w), 722(w), 616(w), 574(m), 517(w), 493(m), 472(w), 446(w), 377(w), 339(w).

Synthesis of [Cu(4-pmp)(H_2O)] (2)

A mixture of $Cu(NO_3)_2 \cdot 3H_2O$ (0.2 mmol, 0.0483 g) and 4-pmpH_2 (0.2 mmol, 0.0342 g) in 8 mL H_2O, adjusted by NaOH (1.0 M) to 4.0, was kept in a Teflon-lined autoclave at 110 °C for 72 h. After the autoclave is cooled to room temperature, blue block-like crystals of compound **2** were collected as a single phase, judged by the powder X-ray diffraction measurement. Yield: 14.5 mg (29% based on 4-pmpH_2). Elemental anal. calcd. for $C_6H_8NO_4PCu$: C, 28.52; H, 3.19; N, 5.54%. Found: C, 28.63; H, 3.26; N, 5.59%. IR (KBr, cm^{-1}): 3015(br), 1613(s), 1558(w), 1498(w), 1424(m), 1254(m), 1221(m), 1151(s), 1130(s), 1093(s), 1071(s), 1046(s), 1013(s), 993(s), 954(m), 881(m), 862(w), 851(w), 834(m), 757(w), 719(w), 673(m), 612(w), 558(m), 542(w), 493(m), 469(w), 419(w), 355(w),325(w). Yield: 10 mg (36%).

X-ray crystallographic analysis

Single crystals of dimensions 0.16×0.12×0.06 mm^3 for **1** and 0.32×0.26×0.10 mm^3 for **2** were selected for indexing and intensity data collection at 180 K on a Bruker SMART APEX-II CCD diffractometer equipped with graphite-monochromatized Mo $K\alpha$ (λ = 0.71073Å) radiation. The low temperature was served by an Oxford Cryosystems Series 700 crystream monitored remotely by using the software interface Cryopad. A hemisphere of data was collected in the θ range 2.42-25.99° for **1** and 3.31-30.60° for **2** using a narrow-frame method with scan widths of 0.30° in ω and an exposure time of 10s per frame. Numbers of measured and observed reflections [$I>2\sigma(I)$] are 5294 and 1434 (R_{int}= 0.0246) for **1** and 10154 and 2457 (R_{int}= 0.0339) for **2** respectively. The data were integrated using the Siemens SAINT program.[58] With the intensities corrected for Lorentz factor, polarization, air absorption, and the absorption due to variation in the path length through the detector faceplate. Empirical absorption and extinction corrections were applied.

The structures were solved by direct method using SHELXS-97[62] and further the structures were refined on F^2 by full matrix least-squares using SHELXL-97.[63] All the non-hydrogen atoms were refined anisotropically. All H atoms were refined isotropically. Crystallographic and refinement details are listed in Table 1. Selected bond lengths are given in Tables S1 and S2. CCDC reference numbers: 1045512 and 1045514 correspond to compounds **1** and **2**, respectively.

Table 1 Crystallographic data for compounds **1** and **2**

Compound	**1**	**2**
Empirical formula	$C_6H_6NO_3PCo$	$C_6H_8NO_4PCu$
F. w.	230.02	252.64
Crystal system	Triclinic	Orthorhombic
Space group	P-1	Pbca
a (Å)	5.1360(3)	8.6107(6)
b (Å)	8.5816(5)	9.9794(7)
c (Å)	8.6869(5)	18.6737(12)
α (°)	76.136(4)	90
β (°)	87.027(4)	90
γ (°)	83.209(4)	90
V(Å^3)	369.00(4)	1604.62(19)
Z	2	8
D_c (g/cm^3)	2.070	2.092
μ (mm^{-1})	2.499	2.898
F(000)	230	1016
GOF on F^2	1.002	1.007
R_1, wR_2 [a]	0.0303,	0.0268,
[$I>2\sigma(I)$]	0.0737	0.0673
R_1, wR_2 [a]	0.0364,	0.0344,
(All data)	0.0761	0.0708
(Δρ)max,	0.667,	0.452,
(Δρ)min (eÅ^{-3})	-0.496	-0.756

[a] $R_1 = \Sigma||F_o| - |F_c||/\Sigma|F_o|$, $wR_2 = [\Sigma w(F_o^2 - F_c^2)^2/\Sigma w(F_o^2)^2]^{1/2}$

Results and discussion

Description of Structures

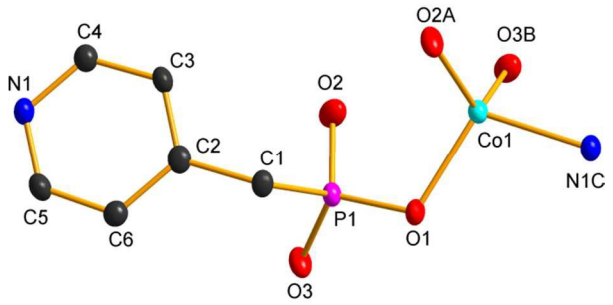

Figure 1 Building unit of **1** with the atomic labeling scheme (50% probability). All H atoms are omitted for clarity. Symmetry codes : A: -x+1,-y,-z+1; B: x+1,y,z; C: x-1,y,z.

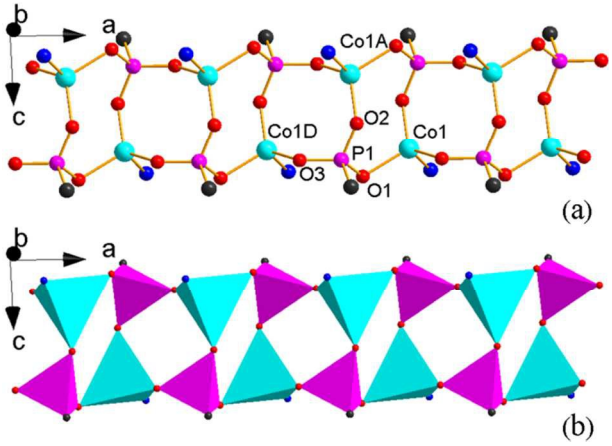

Figure 2 The inorganic chain of structure **1**. Cyan tetrahedron, $CoNO_3$; pink tetrahedron, PO_3C. Symmetry codes : A: -x+1,-y,-z+1; B: x+1,y,z; C: x-1,y,z.

Compound **1** crystallizes in the triclinic lattice with *P*-1 space group. Each asymmetric unit of compound **1** contains one Co^{2+} ion and one 4-pmp^{2-} ligand. As shown in Figure 1, the Co^{2+} ion is four-coordinated by one pyridyl nitrogen atom N1C and three phosphonate oxygen atoms [O1, O2A, O3B] from three equivalent 4-pmp^{2-} ligands. The Co-O(N) bond lengths are in the range of 1.937(2)-2.049(3) Å (Table S1), which are similar to those reported in other Co(II) phosphonates.[45, 51, 55, 58] It is noted that the Co-O bond lengths in tetrahedral coordination environment are shorter than those in octahedral coordination environment.[51, 55] The 4-pmp^{2-} ligand is fully deprotonated. It behaves as a tetradentate metal linker bridging four equivalent Co atoms through three phosphonate oxygen atoms and one pyridyl nitrogen atom. The Co^{2+} ions are bridged by phosphonate group PO_3C (Figure 2a). The Co…Co distances across the O-P-O bridges are 5.136(7) Å for Co1…Co1D, 3.664(6) Å for Co1…Co1A and 4.358(7) Å for Co1A…Co1D. As a result, each $\{PO_3C\}$ tetrahedron is corner-shared with three $\{CoNO_3\}$ tetrahedron and vice versa (Figure 2b), thus forming an inorganic chain running along the *a* axis containing 8-membered rings of $[(Co–O–P–O)_2]$.

The pyridyl groups of 4-pmp^{2-} ligand reside on the two sides of the inorganic chain (Figure S1). The inorganic chains are further connected by organic ligands through phosphonate and pyridyl groups. Consequently, an infinite 2-D layer in the *ab* plane is constructed. The shortest interchain Co…Co distance is 8.581(8) Å. The adjacent pyridyl rings of the 4-pmp^{2-} ligands are parallel, and the distance between them is 3.3158 Å (Figure S2). It is within the range of π–π stacking interactions (3.3–3.8 Å), hence these layers are packed along the *c*-axis through π–π stacking interactions and van der Waals interactions (Figure 3).

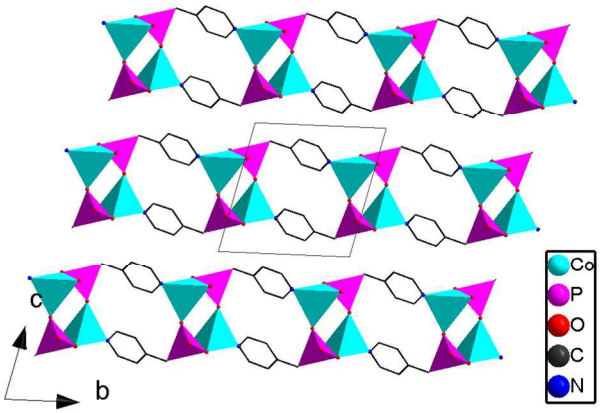

Figure 3 Packing diagram of structure **1** viewed along the *a*-axis. All H atoms are omitted for clarity.

Compound **2** crystallizes in the orthorhombic lattice with *P*bca space group. Figure 4 shows the building unit of compound **2**. The asymmetric unit consists of one Cu^{2+}, one 4-pmp^{2-} ligand and one coordination water molecule. The Cu^{2+} ion has a distorted square-pyramidal coordination environment. The basal positions are filled with three phosphonate oxygen atoms [O1, O2B, O3A] from three equivalent 4-pmp^{2-} ligands and one coordinated water molecule [O4]. The Cu-O bond lengths are in the range from 1.957(1) to 1.993(2) Å (Table S2), respectively. The apical position is occupied by the pyridyl nitrogen [N1C], presenting elongated Cu-N1C bond length [2.232(1) Å], which are similar to those reported in other Cu(II) phosphonates.[43, 50]

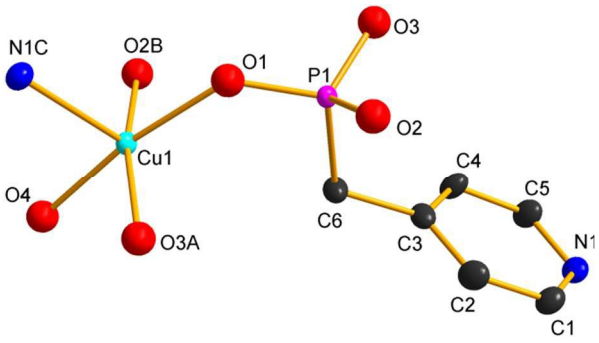

Figure 4 Building unit of **2** with the atomic labeling scheme (50% probability). All H atoms were omitted for clarity. Symmetry codes: A: x+1/2,y,-z+3/2; B: -x,y-1/2,-z+3/2; C: x,-y+3/2,z+1/2.

The 4-pmp^{2-} ligand adopts the same coordination mode as that in compound **1**. The corner-shared connection of $\{PO_3C\}$ tetrahedra and $\{CuNO_4\}$ square pyramids results in an inorganic layer

containing 12-membered rings of [(Cu-O-P-O)$_3$] (Figure 5a). The Cu…Cu distances across the O-P-O bridges are 4.927(4) Å for Cu1…Cu1D, 6.1584 Å for Cu1…Cu1B and 5.242(4) Å for Cu1B…Cu1D (Figure 5b). The inorganic layers are covalently linked by the pyridyl groups of the ligand, resulting in a new type pillared layered of structure (Figure 6). The distance between neighboring layers is 9.3368 Å.

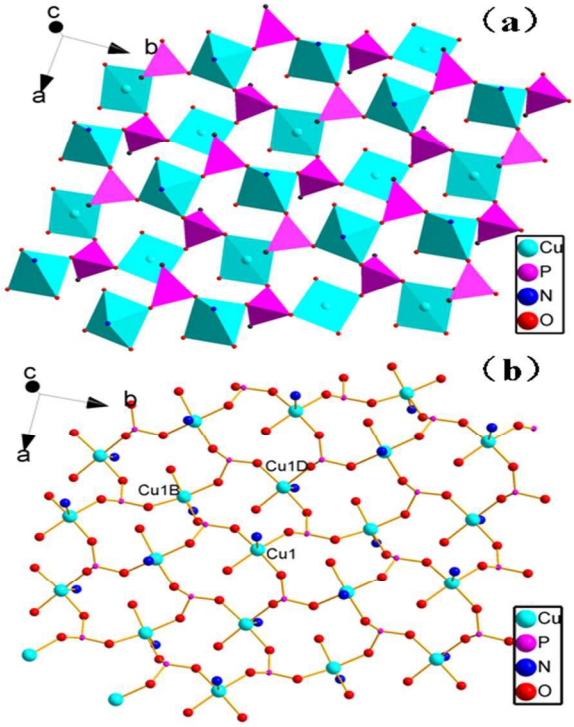

Figure 5 The inorganic layer structure of **2**. Cyan polyhedron, $CuNO_4$; pink tetrahedron, PO_3C. Symmetry codes: A: x+1/2,y,-z+3/2; B: -x,y-1/2,-z+3/2; C: x,-y+3/2,z+1/2.

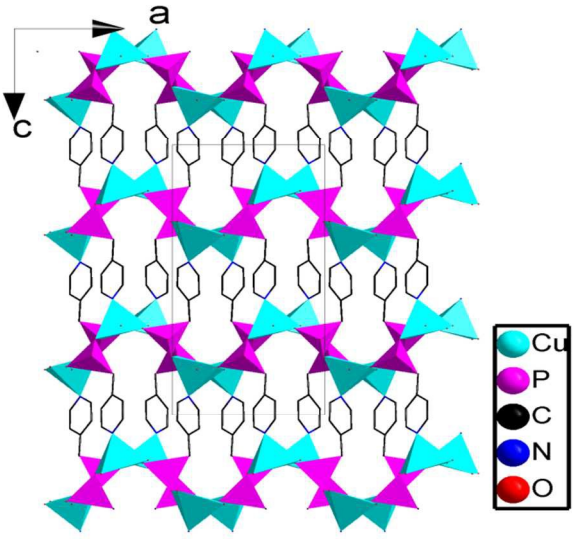

Figure 6 Packing diagram of structure **2,** viewed along the *b*-axis. All H atoms are omitted for clarity

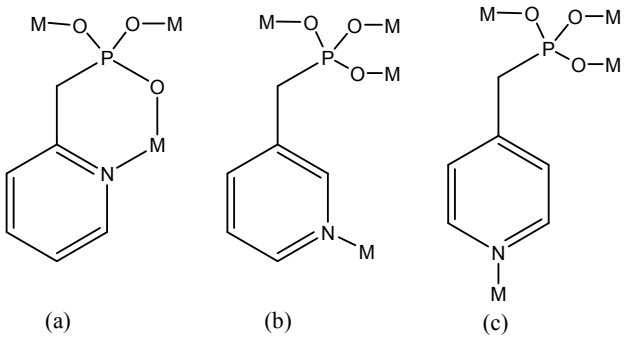

Scheme 2 Coordination modes of 2/3/4-pmp^{2-} ligand.

It is well known that the structures of metal phosphonates are highly dependent on the coordination modes of both ligands and metal ions. Indeed, the different substitution position of pyridylmethylphosphonate ligands (2/3/4-pmp) have different coordination modes when they bind different transition metals. The 2-pmp^{2-} ligand adopts tetradentate bridging coordination mode[51 53] (Scheme 2a), where it acts in a μ_4-η^2N,O, η^1O′, η^1O″ fashion chelating one metal center and bridging other two equivalent metal centers, respectively. The 3-pmp^{2-} ligand adopts tetradentate bridging coordination mode[58] (Scheme 2b), where it acts in a μ_4-η^1N, η^1O, η^1O′, η^1O″ fashion bridging four equivalent metal centers, respectively. The coordination mode of 4-pmp^{2-} in compounds **1** and **2** is similar to 3-pmp^{2-} ligand. In the two compounds, the 4-pmp^{2-} ligand adopts a tetradentate bridging coordination mode too (Scheme 2c). This may explain why layer structures are found in compounds M(2-pmp)(H$_2$O)$_n$[51,53] using the 2-pmp^{2-} ligand, while pillared-layer or layer structures are observed in compounds Co(3-pmp)[58] and **1-2** using 3-pmp^{2-} and 4-pmp^{2-} ligands, respectively.

It is noted that compound **1** and Co(2-pmp),[51] compound **2** and Cu(2-pmp)(H$_2$O)[53] were synthesized under similar conditions, respectively. Although all have similar molecular composition, two types of structures are obtained depending on the different ligands. Compound **1** shows a layer structure constructed from inorganic chains connected by 4-pmp^{2-} ligand, while Co(2-pmp) forms a layer structure in which the {CoNO$_3$} tetrahedron is corner-shared with three {PO$_3$C} tetrahedra and vice versa. Compound **2** features a 3-D pillared-layered structure, while Cu(2-pmp)(H$_2$O) displays a 2-D layer structure. Such a structural difference could be attributed to different coordinated mode of ligand that caused by the phosphonates group position on pyridyl group.

To further understand the topological structures of the two novel metal phosphonates, we examined the connection mode of the metal centers and organic ligands. Each crystallographically independent metal centre is taken as a node, with intermetal bridges ensured by the bridging ligand. In compounds **1** and **2**, each metal center is linked by three phosphonate oxygen atoms and one pyridyl nitrogen atom from four different 4-pmp^{2-} ligands, and each 4-pmp^{2-} ligand also bridges with four metal centers, thus both metal center and P atoms are considered as tetrahedral 4-connected nodes. On the basis of topological analysis carried out with the TOPOS 4.0 program,[65] the structures of these compounds can be described as a uninodal 4-connected 2-D network with a point group symbol of {4^3.6^3} for **1**

(Figure S3) and a uninodal 4-connected 3-D network with a point group symbol of $\{4.6^5\}$ for **2** (Figure S4).

PXRD and thermal stability

The experimental and simulated powder X-ray diffraction (PXRD) patterns of complexes **1** and **2** are shown in Figures S5 and S6. The experimental PXRD patterns at room temperature are in good agreement with the simulated ones based on single-crystal X-ray solution, indicating the phase purity of the bulk products. The differences in reflection intensities are probably due to the preferred orientation effects.

Thermal analyses were carried out for **1** and **2** to examine the thermal stabilities of these complexes (Figure S7). The TG curves of **1** show a stable stage from 25 to 500 °C which indicates that there are no coordination and lattice water molecules. The weight loss above 500 °C is due to the decomposition of the organic ligands and the collapse of the lattice structure. Compound **2** is stable from 25 to 200 °C. The weight loss in the temperature range 200–280 °C is 6.6% which agrees well with that calculated for the release of one coordinated water molecule (calcd. 7.1%). The weight loss above 280 °C is due to the decomposition of the organic ligands and the collapse of the lattice structure. The final products were not characterized in those two cases.

Magnetic property

The magnetic properties of the two compounds were investigated using polycrystalline samples. Figure 7 shows $\chi_M T$ vs. T plots of compound **1**, where χ_M is the molar magnetic susceptibilities measured under a dc field of 1000 Oe. At room temperature, the $\chi_M T$ is 2.86 cm^3 mol^{-1} K, which is approaching the value of 2.70 cm^3 mol^{-1} K expected for tetrahedral Co^{2+} ions with S = 3/2 and g = 2.4.[66] Upon cooling, the value decreases slowly until ca. 30 K, below which the $\chi_M T$ has a steep decrease. This behavior is due to the antiferromagnetic coupling between the neighbouring Co^{2+} ions mediating through O-P-O bridges. Above 100 K, the susceptibility data follows the Curie-Weiss law with the Curie (C) and Weiss constants (θ) of 3.15 cm^3 mol^{-1} K and -30.2 K, respectively (Figure S8). The negative Weiss constant is attributed to the antiferromagnetic (AF) exchange couplings between the Co2+ ions via O-P-O bridges and/or the zero-field splitting effect of the single ion. The sharp peak in the χ_M vs. T plots around 8.0 K suggests an antiferromagnetic ground state of the compound. The ac magnetic susceptibility measurements in the temperature range of 2.0-15.0 K reveal a round peak at ca. 8.0 K which is frequency independent. The appearance of the in-phase peak and the absence of the out-of-phase signals confirm the AF ground state of compound **1** at low temperature. (Figure S9).

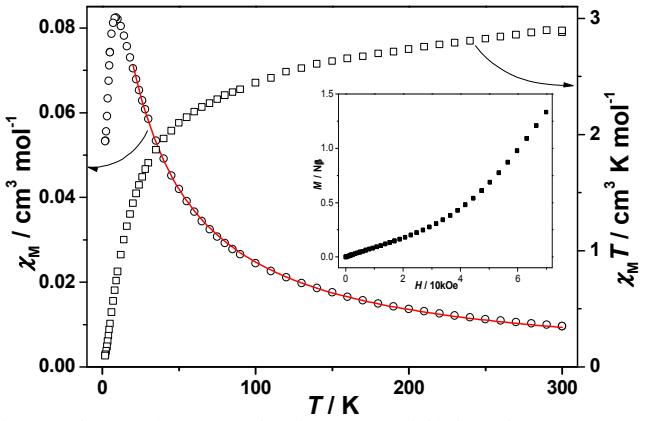

Figure 7 The χ_M and $\chi_M T$ vs T plots for **1**. Inset: Field-dependent magnetization for **2** at 1.8 K

Since the Co^{2+} ions in structure **1** are purely bridged by the O-P-O units which usually can mediate very weak AF interactions, the magnetic behaviour of compound 1 can be viewed as mainly a single ion behavior. For Co^{2+} ion in a tetrahedral environment, the ground state is $^4A_2$ and the first excited state is $^4T_2$. The spin degeneracy of the $^4A_2$ ground state could be removed by the combined effect of the spin–orbit interaction and low symmetry ligand field components, leading to two Kramers doublets with spin S = ±3/2 and S = ±1/2.[43,55,67] Hence, the magnetic susceptibility data of **1** can be analyzed by expression for a noninteracting spin of S = 3/2 using Hamiltonian: [67]

$$\hat{H}=g_u\beta\vec{S}_u\vec{H}_u + D[\hat{S}_z^2 - S(S+1)/3] + E(\hat{S}_x^2 - \hat{S}_y^2)$$

with equations

$$\chi_z = \frac{Ng_z^2\beta^2}{4kT}\frac{1+9\exp(-2D/kT)}{1+\exp(-2D/kT)}$$

$$\chi_x = \frac{Ng_x^2\beta^2}{kT}\frac{1+\frac{3}{4}\frac{kT}{D}-\frac{3}{4}\frac{kT}{D}\exp(-2D/kT)}{1+\exp(-2D/kT)}$$

$$\chi'_M = (\chi_z + 2\chi_x)/3$$

$$\chi_M = \chi'_M/(1-zJ'\chi'_M)$$

where N, k, β have their usual meanings. D is the zero-field splitting energy. The weak magnetic interactions between magnetic centers through O–P–O bridges are accounted (zJ'). Assuming $g_x = g_z = g$, the best fit is obtained in the temperature range 300–20 K, leading to parameters g = 2.5, zJ' = -6.9 cm^{-1}, D = 11.3 cm^{-1} (Figure 7). The zJ' and D value is comparable to those reported for the other cobalt phosphonates containing tetrahedral Co^{2+} ions (ca. -2.5 K)[55].

The isothermal magnetization of compound **1** shown in Figure 7 was measured at 1.8 K. Below 30 kOe, the magnetization increases almost linearly with the applied field, consistent with the AF ground state. However, above 30 kOe the magnetization increases more rapidly. This incomplete S-shaped M vs. H plot suggests a field-

induced phase transition, i.e. metamagnetism. At 70 kOe, the *M* value is 1.33 *Nβ*, which is much lower than the saturated value of 1.5 *Nβ* for (S = 3/2, g = 2.0). The critical field, determined by the peak in the *dM/dH* plot, is about 70 kOe (Figure S10).

Figure 8 exhibits the $\chi_M T$ vs. *T* plots of compound **2**. At 300 K the $\chi_M T$ value is 0.54 cm^3 mol^{-1} K, which is slightly larger than the expected value for non-interacting Cu^{2+} ions with $S = 1/2$ and $g = 2.2$.[54] The value almost keeps constant upon cooling to *ca*. 50 K, after which the $\chi_M T$ reduces to a minimum of 0.13 cm^3 mol^{-1} K at 1.8 K, attributed to the interlayer antiferromagnetic interaction. The Curie (*C*) and Weiss constants (θ) based on the data above 100 K are 0.55 cm^3 mol^{-1} K and -0.73 K, respectively (Figure S11). The small negative Weiss constant indicates the presence of very weak antiferromagnetic interaction in the compound. The χ_M vs. *T* plot measured at 1.0 kOe shows a peak at 3.5 K indicating an antiferromagnetic ground state, which is confirmed by the ac measurements, showing frequency-independent peaks of in-phase signals at 3.5 K without any out-of-phase signals (Figure 12).

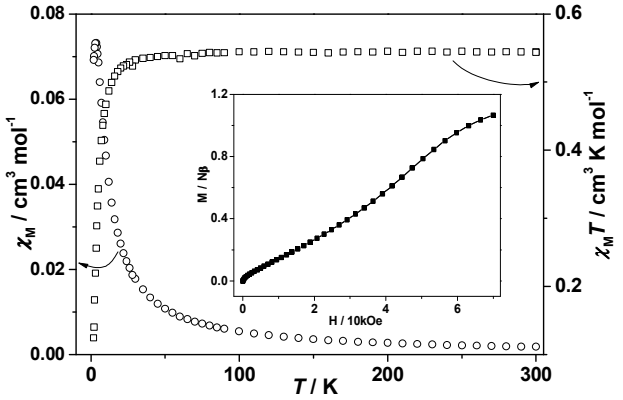

Figure 8 The χ_M and $\chi_M T$ vs *T* plots for **2**. Inset: Field-dependent magnetization for **2** at 1.8 K

The *M* vs. *H* plot of compound **2** was measured at 1.8 K (Figure 8). At low field (< 1 kOe), the magnetization increases steeply with the applied field. Then the *M* increases linearly with the field until to ca. 27 kOe, above which the curve deviates from the line showing *S* shape. This trend of the plot is indicative of a metamagnetic behaviour. The *M* value at 70 kOe is 1.07 *Nβ* which is close to the saturation value. By plotting the *dM/dH* vs. *H*, the critical field (H_c) of the phase transition is estimated as ca. 47.4 kOe at 1.8 K (Figure S13). In the reported metamagnetic compounds, most of them focused on cobalt compound[49,51-56] and only a few copper phosphonate[50] were reported. So it could provide good examples for understanding some interesting metamagnetic phenomena.

Conclusions

In conclusion, we report the syntheses, structures and magnetic properties of two new metal phosphonates based on 4-pmpH_2 linker, namely, [Co(4-pmp)] (**1**) and [Cu(4-pmp)(H_2O)] (**2**). Compound **1** features a two-dimensional layer structure with inorganic chains connected by 4-pmp^{2-} ligand, while compound **2** displays a three-dimensional framework structure in which the inorganic layers are pillared by the pyridyl groups of the ligand. Magnetic measurements reveal that compounds **1** and **2** display a metamagnetic behavior at low temperature.

Acknowledgements

We thank Fundação para a Ciência e a Tecnologia (FCT), FEDER, QREN, COMPETE (PEst-C/CTM/LA0011/2013) and (FCT: SFRH/BPD/74582/2010) for financial support. F.-N. SHI acknowledges FCT for the project of PTDC/CTM-NAN/119994/2010. T.-H. Yang acknowledges the NSF of Jiangsu Province (BK20140244), The Project Sponsored by the Scientific Research Foundation for Returned Overseas Chinese Scholars of State Education Ministry, the NSF for Universities in Jiangsu Province (No. 13KJB150013) and the Changzhou Sci&Tech Program (Grant No. CJ20140031).

Notes and references

[a] School of Chemistry & Environmental Engineering, Jiangsu University of Technology, Changzhou 213001, P. R. China.
[b] School of Science, Shenyang University of Technology, Shenyang 110870, P. R. China. E-mail: fshi96@foxmail.com.
[c] State Key Laboratory of Coordination Chemistry, School of Chemistry & Chemical Engineering, Nanjing University, Nanjing 210093, P. R. China. E-mail: lmzheng@nju.edu.cn
[d] Department of Chemistry, CICECO, University of Aveiro, 3810-193 Aveiro, Portugal.

† Electronic Supplementary Information (ESI) available: topological structrue, PXRD, TG, magnetic data and table of selected bond lengths and angles. CCDC 1045512 and 1045514. For ESI and crystallographic data in CIF or other format see DOI: 10.1039/b000000x/

1 A. Clearfield, *Metal phosphonate chemistry*: *From Synthesis to Application*, Royal Society of Chemistry, Oxford, U. K., 2012.
2 K. J. Gagnon, H. P. Perry and A. Clearfield, *Chem. Rev.*, 2012, **112**, 1034-1054.
3 D. S. Li, Y. P. Wu, J. Zhao, J. Zhang and J. Y. Lu, *Coord. Chem.Rev.*, 2014, **261**, 1-27.
4 H. Li, Z. J. Yao, D. Liu and J. G. X. Jin, *Coord. Chem.Rev.*, 2015, **293**, 139-157.
5 M. T. Wharmby, J. P. S. Mowat, S. P. Thompson and P. A.Wright, *J. Am. Chem. Soc.*, 2011, **133**, 1266-1269.
6 S. R. Miller, G. M. Pearce, P. A. Wright, F. Bonino, S. Chavan, S. Bordiga, I. Margiolaki, N. Guillou, G. Feerey, S. Bourrelly and P. L. Llewellyn, *J. Am. Chem. Soc.*, 2008, **130**, 15967-15981.
7 E. Brunet, H. M. H. Alhendawi, C. Cerro, M. J. de la Mata, O. Juanes and J. C. Rodriguez-Ubis, *Angew. Chem. Int. Ed.*, 2006, **45**, 6918-6920.
8 L. Q. Ma, C. Abney and W. B. Lin, *Chem. Soc. Rev.*, 2009, **38**, 1248-1256.
9 W. J. Youngblood, S. H. A. Lee, Y. Kobayashi, E. A. Hernandez-Pagan, P. G. Hoertz, T. A. Moore, A. L. Moore, D. Gust and T. E. Mallouk, *J. Am. Chem. Soc.*, 2009, **131**, 926-927.

10 S. Chessa, N. J. Clayden, M. Bochmann and J. A. Wright, *Chem. Commun.*, 2009, 797-799.
11 S. S. Bao, L. F. Ma, Y. Wang, L. Fang, C. J. Zhu, Y. Z. Li and L. M. Zheng, *Chem.-Eur. J.*, 2007, **13**, 2333-2343.
12 S.-S. Bao, K. Otsubo, J. M. Taylor, Z. Jiang, L.-M. Zheng and H. Kitagawa, *J. Am. Chem. Soc.*, 2014, **136**, 9292-9295.
13 M. Bazaga-Garcia, R. M. P. Colodrero, M. Papadaki, P. Garczarek, J. Zon, P. Olivera-Pastor, E. R. Losilla, L. Leon-Reina, M. A. G. Aranda, D. Choquesillo-Lazarte, K. D. Demadis and A. Cabeza, *J. Am. Chem. Soc.*, 2014, **136**, 5731-5739.
14 R. M. P. Colodrero, K. E. Papathanasiou, N. Stavgianoudaki, P. Olivera-Pastor, E. R. Losilla, M. A. G. Aranda, L. Leon-Reina, J. Sanz, I. Sobrados, D. Choquesillo-Lazarte, J. M. Garcia-Ruiz, P. Atienzar, F. Rey, K. D. Demadis and A. Cabeza, *Chem. Mater.*, 2012, **24**, 3780-3792.
15 F. Costantino, A. Donnadio and M. Casciola, *Inorg. Chem.*, 2012, **51**, 6992-7000.
16 S. Begum, Z. Y. Wang, A. Donnadio, F. Costantino, M. Casciola, R. Valiullin, C. Chmelik, M. Bertmer, J. Karger, J. Haase and H. Krautscheid, *Chem.-Eur. J.*, 2014, **20**, 8862-8866.
17 J. G. Mao, *Coordin. Chem. Rev.*, 2007, **251**, 1493-1520.
18 E. Brunet, H. M. H. Alhendawi, O. Juanes, L. Jimenez and J. C. Rodriguez-Ubis, *J. Mater. Chem.*, 2009, **19**, 2494-2502.
19 X. G. Liu, K. Zhou, J. Dong, C. J. Zhu, S. S. Bao and L. M. Zheng, *Inorg. Chem.*, 2009, **48**, 1901-1905.
20 S. Maheswaran, G. Chastanet, S. J. Teat, T. Mallah, R. Sessoli, W. Wernsdorfer and R. E. P. Winpenny, *Angew. Chem. Int. Ed.*, 2005, **44**, 5044-5048.
21 M. Shanmugam, G. Chastanet, T. Mallah, R. Sessoli, S. J. Teat, G. A. Timco and R. E. P. Winpenny, *Chem.-Eur. J.*, 2006, **12**, 8777-8785.
22 S. Langley, M. Helliwell, R. Sessoli, S. J. Teat and R. E. P. Winpenny, *Inorg. Chem.*, 2008, **47**, 497-507.
23 J. A. Sheikh, A. Adhikary, H. S. Jena, S. Biswas and S. Konar, *Inorg. Chem.*, 2014, **53**, 1606-1613.
24 V. Baskar, K. Gopal, M. Helliwell, F. Tuna, W. Wernsdorfer and R. E. P. Winpenny, *Dalton. Trans.*, 2010, **39**, 4747-4750.
25 Y. S. Ma, Y. Song, Y. Z. Li and L. M. Zheng, *Inorg. Chem.*, 2007, **46**, 5459-5461.
26 Y. S. Ma, Y. Z. Li, Y. Song and L. M. Zheng, *Inorg. Chem.*, 2008, **47**, 4536-4544.
27 M. Ren, S. S. Bao, N. Hoshino, T. Akutagawa, B. W. Wang, Y. C. Ding, S. Q. Wei and L. M. Zheng, *Chem.-Eur. J.*, 2013, **19**, 9619-9628.
28 T. T. Wang, M. Ren, S. S. Bao and L. M. Zheng, *Eur. J. Inorg. Chem.*, 2014, **2014**, 1042-1050.
29 M. Ren, S. S. Bao, R. A. S. Ferreira, L. M. Zheng and L. D. Carlos, *Chem. Commun.*, 2014, **50**, 7621-7624.
30 D. Zeng, M. Ren, S. S. Bao, L. Li and L. M. Zheng, *Chem. Commun.*, 2014, **50**, 8356-8359.
31 Z. M. Sun, A. V. Prosvirin, H. H. Zhao, J. G. Mao and K. R. Dunbar, *J. Appl. Phys.*, 2005, **97**, 10B305.
32 J. T. Brockman, T. C. Stamatatos, W. Wernsdorfer, K. A. Abboud and G. Christou, *Inorg. Chem.*, 2007, **46**, 9160-9171.
33 T. T. Wang, M. Ren, S. S. Bao, B. Liu, L. Pi, Z. S. Cai, Z. H. Zheng, Z. L. Xu and L. M. Zheng, *Inorg. Chem.*, 2014, **53**, 3117-3125.
34 A. V. Palii, S. M. Ostrovsky, S. I. Klokishner, O. S. Reu, Z. M. Sun, A. V. Prosvirin, H. H. Zhao, J. G. Mao and K. R. Dunbar, *J. Phys. Chem. A*, 2006, **110**, 14003-14012.
35 A. V. Palii, O. S. Reu, S. M. Ostrovsky, S. I. Klokishner, B. S. Tsukerblat, Z. M. Sun, J. G. Mao, A. V. Prosvirin, H. H. Zhao and K. R. Dunbar, *J. Am. Chem. Soc.*, 2008, **130**, 14729-14738.
35 Z. C. Zhang and L. M. Zheng, *Inorg. Chem. Commun.*, 2008, **11**, 1243-1245.
36 D. K. Cao, X. J. Xie, Y. Z. Li and L. M. Zheng, *Dalton. Trans.*, 2008, 5008-5015.
38 P. F. Wang, D. K. Cao, S. S. Bao, H. J. Jin, Y. Z. Li, T. W. Wang and L. M. Zheng, *Dalton. Trans.*, 2011, **40**, 1307-1312.
39 P. F. Wang, Y. Duan, J. M. Clemente-Juan, Y. Song, K. Qian, S. Gao and L. M. Zheng, *Chem.-Eur. J.*, 2011, **17**, 3579-3583.
40 D. S. Li, J. Zhao, Y. P. Wu, B. Liu, L. Bai, K. Zou and M. Du, *Inorg. Chem.*, 2013, **52**, 8091-8098.
41 S. O. H. Gutschke, D. J. Price, A. K. Powell and P. T. Wood, *Angew. Chem. Int. Ed.*, 1999, **38**, 1088-1090.
42 C. Bellitto and F. Federici, *Inorg. Chem.*, 2002, **41**, 709-714.
43 D. Y. Kong, Y. Li, O. Y. Xiang, A. V. Prosvirin, H. H. Zhao, J. H. Ross, K. R. Dunbar and A. Clearfield, *Chem. Mater.*, 2004, **16**, 3020-3031.
44 B. P. Yang, A. V. Prosvirin, Y. Q. Guo and J. G. Mao, *Inorg. Chem.*, 2008, **47**, 1453-1459.
45 T. H. Zhou, Z. Z. He, X. Xu, X. Y. Qian and J. G. Mao, *Cryst. Growth Des.*, 2013, **13**, 838-843.
46 Y. S. Ma, Y. Song, W. X. Du, Y. Z. Li and L. M. Zheng, *Dalton. Trans.*, 2006, 3228-3235.
47 D. K. Cao, Y. Z. Li and L. M. Zheng, *Inorg. Chem.*, 2007, **46**, 7571-7578.
48 L. R. Guo, F. Zhu, Y. Chen, Y. Z. Li and L. M. Zheng, *Dalton. Trans.*, 2009, 8548-8554.
49 P. Yin, S. Gao, L. M. Zheng, Z. M. Wang and X. Q. Xin, *Chem. Commun.*, 2003, 1076-1077.
50 L. M. Zheng, S. Gao, H. H. Song, S. Decurtins, A. J. Jacobson and X. Q. Xin, *Chem. Mater.*, 2002, **14**, 3143-3147.
51 T. H. Yang, Y. Liao, L. M. Zheng, R. E. Dinnebier, Y. H. Su and J. Ma, *Chem. Commun.*, 2009, 3023-3025.
52 T. H. Yang, E. S. Knowles, D. M. Pajerowski, J. S. Xia, L. A. Yin, S. Gao, M. W. Meisel and L. M. Zheng, *Inorg. Chem.*, 2010, **49**, 8474-8480.
53 T. H. Yang, D. K. Cao, T. W. Wang and L. M. Zheng, *Inorg. Chem. Commun.*, 2010, **13**, 1558-1561.
54 P. F. Wang, S. S. Bao, S. M. Zhang, D. K. Cao, X. G. Liu and L. M. Zheng, *Eur. J. Inorg. Chem.*, 2010, 895-901.
55 S. Z. Hou, D. K. Cao, X. G. Liu, Y. Z. Li and L. M. Zheng, *Dalton. Trans.*, 2009, 2746-2750.
56 D. K. Cao, M. J. Liu, J. A. Huang, S. S. Bao and L. M. Zheng, *Inorg. Chem.*, 2011, **50**, 2278-2287.
57 T. H. Yang, D. K. Cao, Y. Z. Li and L. M. Zheng, *J. Solid State Chem.*, 2010, **183**, 1159-1164.
58 R. Sen, D. Saha, D. Mal, P. Brandao, G. Rogez and Z. Lin, *Eur. J. Inorg. Chem.*, 2013, 5020-5026.
59 A. Zavras, J. A. Fry, C. M. Beavers, G. H. Talbo and A. F. Richards, *CrystEngComm*, 2011, **13**, 3551-3561.
60 C. R. Samanamu, M. M. Olmstead, J. L. Montchamp and A. F. Richards, *Inorg. Chem.*, 2008, **47**, 3879-3887.
61 *SAINT+, Data Integration Engine, v. 7.23a*, Bruker AXS, Madison, Wisconsin, 1997-2005.
62 G. M. Sheldrick, *SHELXL-97, Program for Crystal Structure Solution*, University of Göttingen, Germany, 1997.

63 G. M. Sheldrick, *SHELXL-97, Program for Crystal Structure Refinement*, University of Göttingen, Germany, 1997.
64 D. K. Cao, Y. Z. Li, Y. Song and L. M. Zheng, *Inorg. Chem.*, 2005, **44**, 3599-3604.
65 V. A. Blatov and A. P. Shevchenko, *TOPOS 4.0*, Samara State Universty, Samara Oblast, Russia, 2008.
66 M. Kurmoo, *Chem. Soc. Rev.*, 2009, **38**, 1353-1379.
67 O. Kahn, *Molecular Magnetism*, VCH Publishers, New York, 1993.

Synopsis

Compounds [Co(4-pmp)] (**1**) and [Cu(4-pmp)(H_2O)] (**2**) (4-pmp = 4-pyridylmethylphosphonate) with 2-D and 3-D structures are synthesized and characterized, which show metamagnetism at low temperature.